CHEMBIOCHEM

DOI: 10.1002/cbic.201000402

Using the Peptide Bp100 as a Cell-Penetrating Tool for the Chemical Engineering of Actin Filaments within Living Plant Cells

Kai Eggenberger,*[a] Christian Mink,[b] Parvesh Wadhwani,[b] Anne S. Ulrich,[b] and Peter Nick[a]

The delivery of externally applied macromolecules or nanoparticles into living cells still represents a critically limiting step before the full capabilities of chemical engineering can be explored. Molecular transporters such as cell-penetrating peptides, peptoids, and other mimetics can be used to carry cargo across the cellular membrane, but it is still difficult to find suitable sequences that operate efficiently for any particular type of cell. Here we report that BP100 (KKLFKKILKYL-amide), originally designed as an antimicrobial peptide against plant pathogens, can be employed as a fast and efficient cell-penetrating agent to transport fluorescent test cargoes into the cytosol of walled plant cells. The uptake of BP100 proceeds slightly more slowly than the endocytosis of fluorescent dextranes, but BP100 accumulates more efficiently and to much higher levels (by an order of magnitude). The entry of BP100 can be efficiently blocked by latrunculin B; this suggests that actin filaments are essential to the uptake mechanism. To test whether this novel transporter can also be used to deliver functional cargoes, we designed a fusion construct of BP100 with the actin-binding Lifeact peptide (MGVADLIKKFESISKEE). We demonstrated that the short BP100 could transport the attached 17-residue sequence quickly and efficiently into tobacco cells. The Lifeact construct retained its functionality as it successfully labeled the actin bundles that tether the nucleus in the cell center.

Introduction

Cell-penetrating peptides (CPPs) and their synthetic analogues, such as β-peptides or peptoids, have attracted considerable attention due to their ability to deliver functionally active cargo like RNA, DNA, drugs, antibodies, and nanoparticles into cells in a nondestructive manner.[1–3] CPPs tend to be short cationic peptides with an amphiphilic character that are attracted by the anionic cell surface and can eventually penetrate through the hydrophobic lipid bilayer. Despite a lot of effort to elucidate the mechanism of membrane penetration, this process is still poorly understood, yet it seems to be independent of classical receptor-mediated pathways and might, in some cases, involve endocytosis as an initial step.[4–6]

Most studies have concentrated on the application of CPPs to mammalian cells and have shown that the uptake efficiency of different peptides varies considerably with the type of cell. With a view to the chemical engineering of plants, several conventional CPPs have been explored with some success, for example, arginine-rich TAT analogues, transportan, penetratin, and pVec.[7–11] In previous work, we successfully used peptoids to deliver a fluorescent cargo into intact, walled plant cells.[12] Peptoids are resistant to protease degradation, which is especially important in plant cells with their huge vacuole filled with hydrolytic enzymes. A drawback of peptoids is their difficult synthesis and the fact that they are not accessible for recombinant expression. We therefore explored the performance of peptides as vehicles to introduce functional cargoes into plant cells. Yet, it is evident that a new, optimized generation of peptides will be required for plant cells, as they possess a rigid wall and exhibit a very different membrane composition and intracellular trafficking machinery from animals. Having tried out various membrane-active sequences with low efficiency, the aim of our study was to test a designated plant-compatible peptide as a novel CPP and to demonstrate its efficient uptake and ability to carry a functionally relevant cargo inside.

BP100 (KKLFKKILKYL-amide) is an antimicrobial peptide that has been optimized against plant pathogens. Its sequence was obtained by systematic mutation of Pep3 (WKLFKKILKVL-amide), a hybrid peptide derived from the naturally occurring cecropin-A (an antimicrobial peptide from the moth *Hyalophora cecropia*) and melittin (a membrane-permeabilizing component of bee venom).[13–15] Both BP100 and Pep3 display high antimicrobial activity against plant pathogens such as *Erwinia amylovora*, *Pseudomonas syringae*, and *Xanthomonas vesicatoria*. They share structural similarities with some of the commonly used CPPs in that they are cationic and amphiphilic, but

[a] *K. Eggenberger, Prof. Dr. P. Nick*
Molecular Cell Biology, Institute of Botany
DFG-Center of Functional Nanostructures (CFN)
Karlsruhe Institute of Technology (KIT)
Kaiserstrasse 2, 76131 Karlsruhe (Germany)
Fax: (+49) 721-608-4193
E-mail: kai.eggenberger@kit.edu

[b] *Dr. C. Mink, Dr. P. Wadhwani, Prof. Dr. A. S. Ulrich*
Institute of Biological Interfaces (IBG-2) and CFN, KIT
Institute of Organic Chemistry
Fritz-Haber Weg 6, 76131 Karlsruhe (Germany)

Supporting information for this article is available on the WWW under http://dx.doi.org/10.1002/cbic.201000402.

WILEY ONLINE LIBRARY © 2011 Wiley-VCH Verlag GmbH & Co. KGaA, Weinheim

their potential use as a vector for cellular delivery has not been explored.

To test BP100 as a molecular transporter, we first needed to monitor whether the fluorescent-labeled peptide could per se enter tobacco cells rapidly and efficiently. The next critical question was whether it can carry a cargo along, and whether it would affect cell viability in the long term. Actin is the central element of the cytoskeleton and has important and highly specific functions in eukaryotic cells. While mammalian cells rely on actin filaments for cellular migration and cytokinesis, in plant cells the actin cytoskeleton forms the backbone of inter- and intracellular trafficking.[16] These filaments are also key players in cell division, defense against pathogens, and the polar transport of the plant hormone auxin.[17,18] These functions of actin have been identified from different visualization techniques, such as staining with fluorescent phalloidin or fusion constructs of actin-binding proteins with fluorescent proteins.[19] These techniques have the drawback that they either rely on fixation (in the case of fluorescent phalloidin that otherwise cannot permeate the plasma membrane) or on genetic transformation of the target cell. Thus, for in vivo imaging, novel approaches that require neither fixation nor (time-consuming) transformation and selection steps are highly desirable. Actin filaments make ideal markers to study these criteria, as even subtle effects on the cellular physiology would drastically perturb the structure and functionality of the actin network.[20]

We therefore combined the general aim of finding a plant-compatible CPP with the specific need to apply this tool to chemical engineering of actin filaments. This approach utilizes the recently discovered actin marker peptide "Lifeact" as a cargo, which of itself is only 17 amino acids long (MGVADLIKKFESISKEE).[21] Lifeact was designed from an actin-binding domain that is specific for yeasts and cannot be found in higher eukaryotic cells. It has been successfully used as a powerful marker in different target cells.[22] However, so far, this approach has required genetic engineering that involves transformation and selection of the target cell. In a proof-of-principle approach, we have fused the Lifeact sequence (as functional cargo) to BP100 (as cell-permeating transporter); this allowed us to visualize actin filaments in living, untransformed tobacco BY-2 cells. To our knowledge this is not only the first time that BP100 has been used as a cell-penetrating carrier, but also the first time that actin filaments have been specifically targeted for labeling by a CPP.

Results and Discussion

BP100 accumulates more rapidly and to much higher levels than the endocytotic test cargo FD-4

We first followed the internalization of fluorescein-isothiocyanate (FITC)-labeled BP100 into tobacco BY-2 cells over time by epifluorescence microscopy in combination with optical sectioning by using apotome technology. This approach ensures that the observed signal originates only from the focal plane, and excludes potential out-of-focus fluorescence signals from cell-wall-bound marker that has not been internalized. The fluorescent signal appeared inside the vacuole shortly after the start of incubation and intensified with time. We quantified the uptake of BP100 as described previously and compared the time course and amplitude of uptake with that of the fluorescently labeled 4-kDa dextrane (FD-4), a membrane-impermeable endocytosis tracer.[12,23] As shown in Figure 1 A, FD-4 accumulates only to very low levels, whereas the signal of fluorescent BP100 increases steadily to a much higher plateau around 12 h after the start of incubation (Figure 1). When uptake is plotted relative to the final value recorded after 20 h (Figure 2 A), FD-4 is seen to reach the 50% level after 2 h, whereas BP100 is transported over a much longer period (reaching half-maximum at more than 6 h). When uptake is plotted in absolute values, corrected for the concentration differences of the two fluorophores (25 μM for FD-4, 2.15 μM for BP100; Figure 2 B), it becomes clear that BP100 permeates to a much higher extent than FD-4. Even after just 2 h, BP100 exceeds the endocytosed FD-4 by a factor of 9, and after 20 h, this excess has increased further to a factor of 14. Thus, although it cannot be excluded that some of BP100 could enter cells through the same endocytotic pathway that drives the uptake of FD-4, the major part of BP100 uptake seems to occur by a mechanism other than standard endocytotic turnover.

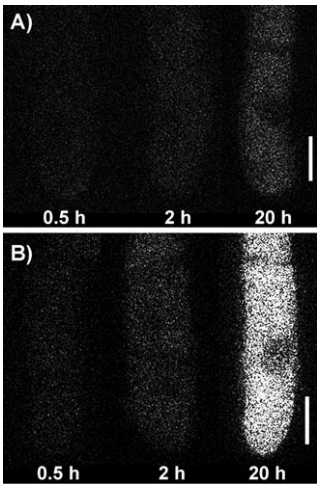

Figure 1. Individual tobacco BY-2 cells at different times after incubation A) with the endocytosis tracer FD-4, and B) with the cell-penetrating peptide BP100. Scale bar = 20 μm.

The uptake of BP100 is enhanced in post-cycling cells

To test whether the amount of BP100 internalized by the tobacco BY-2 cells depends on developmental stage, we monitored uptake during different stages of the cultivation cycle and compared it with that of the endocytosis tracer FD-4. When the uptake (within the first interval of 2 h, and after correction for the increasing cell density) was plotted as a function of cell age, an increase was observed for both FD-4 and BP100 that reached a plateau between four and five days after

 © 2011 Wiley-VCH Verlag GmbH & Co. KGaA, Weinheim

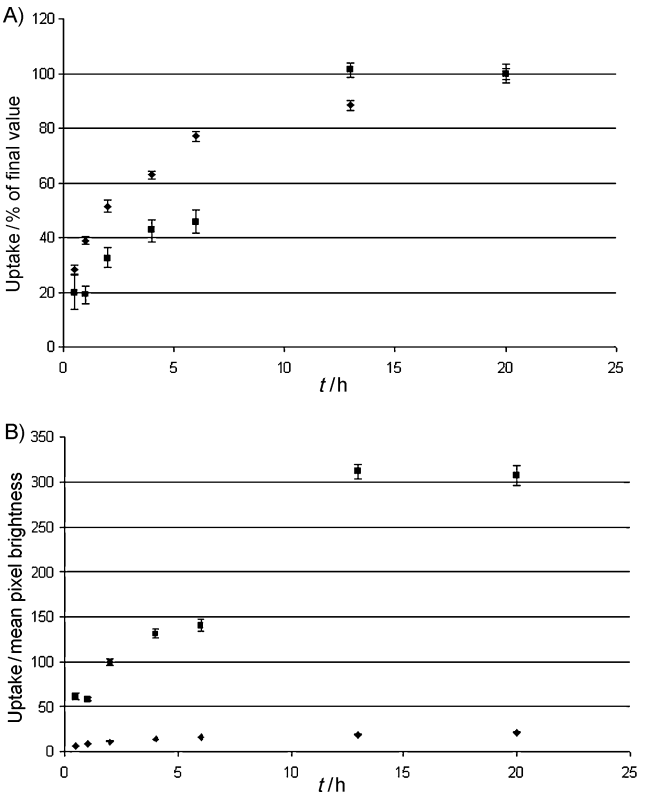

Figure 2. Time course of uptake for the cell-penetrating peptide BP100 (■) and the endocytosis tracer FD-4 (◆). A) Values calculated relative to the final value at 20 h, B) Absolute values adjusted with respect to fluorophore concentration in the incubation medium (25 μM for FD-4, 2.15 μM for BP100). Each data point represents the mean of 178–495 individual cells from two independent experimental series. Error bars indicate standard error: $n = 178–495$

subcultivation (Figure 3). However, from day 3 onwards, the uptake of BP100 progressively exceeded that of FD-4 by about twofold. In tobacco cell lines, a logarithmic phase of vigorous

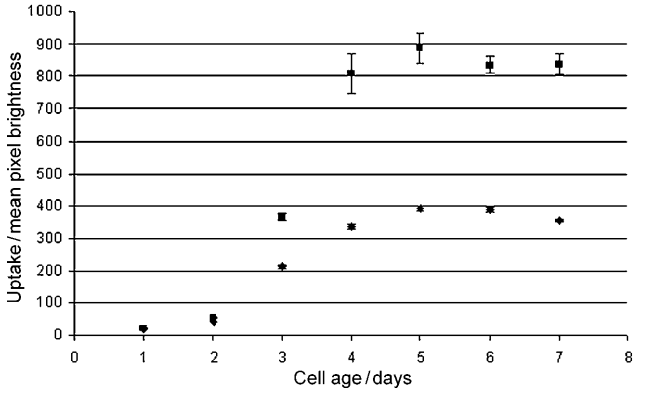

Figure 3. Uptake of the cell-penetrating peptide BP100 (■; 2.15 μM) and the endocytosis tracer FD-4 (◆, 25 μM), depending on the stage of the cultivation cycle indicated as days after subcultivation. Uptake over 2 h was quantified and corrected for the increase in cell density with progression of the culture cycle, but, unlike Figure 2, not with respect to fluorophore concentration to allow both graphs to be compared. Each data point represents the mean of 146–328 individual cells from two independent experimental series. Error bars indicate standard error: $n = 146–328$

cell division is followed by a phase of post-cycling cell expansions that are regulated by different auxin-signaling pathways triggered by different receptors and conveyed by different transduction machineries.[24] In the rapidly growing BY-2 line, the transition from the division to the expansion phase occurs between three and four days after subcultivation. Thus, the increased uptake of BP100 coincides with the transition from division-dependent to expansion-driven growth and with the switch to a different system of auxin-signaling.

The uptake of BP100 is only partially driven by endocytosis

Despite extensive research to elucidate the mechanism of membrane penetration, this process is still poorly understood. To probe for potential factors that influence the unknown mechanism of BP100 uptake, we examined the effect of pH, because it has previously been reported that low pH facilitates protein uptake in mammalian cells.[25] We incubated tobacco BY-2 cells with both FD-4 and BP100 for 2 h in sterile culture medium, in which the pH was either increased or decreased by 1 pH unit compared to the regular pH of 5.8. Uptake of the endocytosis tracer FD-4 decreased by almost 50% under the more neutral, and increased by almost 50% under the more acidic conditions (Figure 4); this is consistent with published

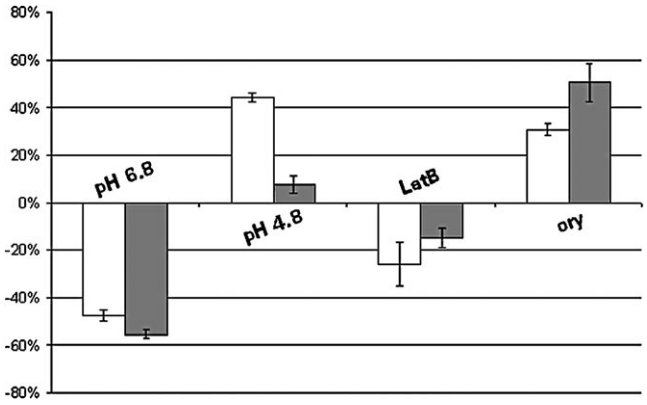

Figure 4. Changes in the uptake of FD-4 (□) and BP100 (■) in comparison to untreated cells. Duration of incubation 2 h; pH 6.8 and 4.8: pH increased or decreased by 1 pH unit; LatB: 500 nM latrunculin B; ory: 5 μM oryzalin.

reports.[25] In contrast, the uptake of BP100, although decreasing similarly at the neutral pH, did not increase significantly at the more acidic pH.

To gain insight into the role of the cytoskeleton in the internalization of FD-4 and BP100, we pretreated the tobacco cells either with latrunculin B, an inhibitor of actin filaments, or with oryzalin, a plant-specific inhibitor of microtubules for 12 h overnight before probing the uptake of BP100 or FD-4 for 2 h. Both drugs act by sequestering the monomers (in the case of actin) or heterodimers (in the case of tubulin), thereby leading to depolymerization of the corresponding cytoskeletal element due to its innate turnover.[26–30] When uptake was quantified after inhibitor treatment, both the endocytosis tracer FD-4 and the fluorescent-labeled peptide BP100 were reduced by latrun-

 © 2011 Wiley-VCH Verlag GmbH & Co. KGaA, Weinheim

culin B. Surprisingly, the elimination of microtubules by oryzalin caused a significant increase in both FD-4 and BP100 within the cells. According to these results, actin seems to be the driving force for uptake, which decreased in the absence of actin filaments. However, the finding that uptake increased when the actin filaments remained the only cytoskeletal component present, suggests that microtubules act as negative regulators of uptake. This effect is independent of the molecular nature of the cargo (FD-4 or BP100), thus suggesting that it invokes an endocytotic component of uptake that is shared by the two cargoes. These results are therefore consistent with published reports that, in plants, actin filaments but not microtubules participate in receptor-mediated endocytosis.[31,32]

BP100 can be targeted to the phragmosome by using the Lifeact motif

After successful delivery of the fluorescent marker FITC by BP100, we explored possible applications of delivering a biofunctional cargo, Lifeact, into tobacco cells in vivo. It has already been shown that the 17-residue sequence of Lifeact binds to actin microfilaments upon stable expression of a fusion construct of Lifeact and a fluorescent protein. We therefore designed two modular peptides (Figure 5), each harboring

RhB-BP100-Lifeact (RBL): RhB - KKLFKKILKYL - MGVADLIKKFESISKEE

RhB-Lifeact-BP100 (RLB): RhB - MGVADLIKKFESISKEE - KKLFKKILKYL

Figure 5. Modular design of the two test peptides, which are each composed of a transport module based on the cell-permeating domain of BP100, a functional module based on the actin-binding Lifeact motif, and a detection module (RhB to report intracellular localization in a background, where actin filaments are labeled by GFP). The peptide RBL was synthesized such that the functional module at the C terminus was free to bind the actin target, whereas the control peptide RBL should serve as a negative control, given that the functional module is masked on both sides.

a transport module based on the CPP BP100, a functional module based on the actin-binding Lifeact motif, plus a detection module (Rhodamin B (RhB) to report intracellular localization in a background, where actin filaments are labeled by green fluorescent protein (GFP)). The two peptides differed in the sequence of these three modules. In RBL (RhB-BP100-Lifeact), the Lifeact sequence was exposed freely at the C terminus, whereas in RLB (RhB-Lifeact-BP100) the Lifeact motif was masked by Rhodamin B at the N terminus and BP100 at the C terminus. While both peptides are assumed to be able to enter tobacco BY-2 cells, only the freely exposed Lifeact motif of the RBL peptide should be able to bind to actin filaments. The RLB peptide, in which Lifeact is placed between the transporter sequence and the fluorescent label, would be expected to serve as a negative control.

In the rapidly cycling BY-2 cells, actin is organized into two major structures: a fine mesh of cortical actin is found adjacent to the cell wall, whereas the nucleus is tethered in the center of the cell by a characteristic "Maltese cross" composed of transvacuolar actin cables, the so-called phragmosome. These actin structures not only differ functionally, but also with respect to their accessory proteins.[33] For instance, the actin cables of the phragmosome are decorated with the plant-specific microtubule motor KCH, which crosslinks actin filaments to microtubules.[34]

Both 28-residue-peptide constructs were able to enter the cells rapidly, but their intracellular distribution differed completely. Whereas the RLB control peptide accumulated in the vacuole and was excluded from the actin cables of the phragmosome (Figure 6), the RBL construct localized in transvacuolar strands and colocalized with the actin cables of the phragmosome. This characteristic distribution of the peptides was observed in untransformed BY-2 cells (Figure 7 A), as well as in the actin-marker line GF-11 (Figure 7 B). The tight colocalization of the RBL peptide with the GFP-tagged actin filaments in the GF-11 line results in a yellow signal when both channels merge (Figure 7 B). Thus, the RBL peptide has been successfully targeted to a subpopulation of the actin cytoskeleton, the phragmosome.

We have recently demonstrated that polyguanidine peptoids are rapidly taken up by tobacco BY-2 cells.[12] The immediate

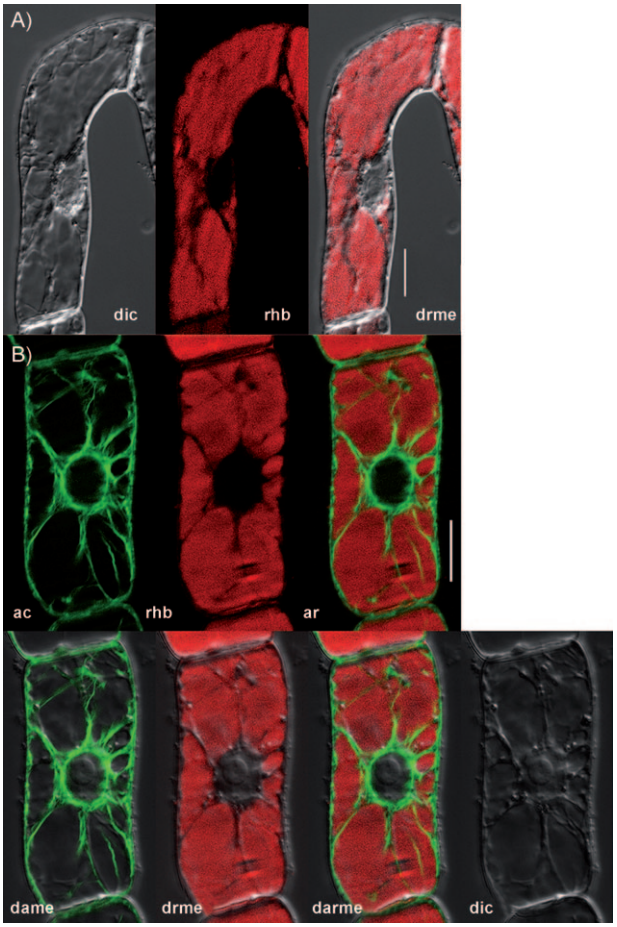

Figure 6. Localization of the control peptide RLB A) in individual cells of untransformed tobacco BY-2 cells and B) in the GF-11 line, where actin filaments are visualized by a GFP-tagged actin-binding protein. dic: differential interference contrast, rhb: signal for the RLB construct, drme: merged dic and rhb signals; this demonstrates that the RLB peptide is able to enter the cells, ac: signal for actin microfilaments, ar: merged actin and RLB signals; this shows that the peptide does not colocalize with the transvacuolar actin cables. Scale bar = 20 μm.

 © 2011 Wiley-VCH Verlag GmbH & Co. KGaA, Weinheim

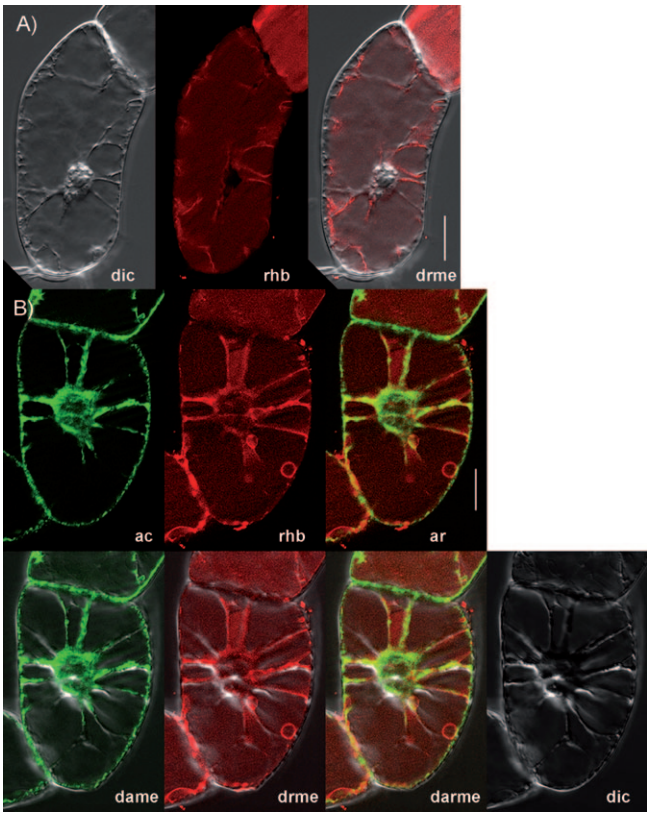

Figure 7. Localization of the RBL peptide A) in individual cells of untransformed tobacco BY-2 cells and B) in the line GF-11, where actin filaments are visualized by a GFP-tagged actin-binding protein. Abbreviations as in Figure 6; the merged actin and RBL signals produce a yellow signal from the strong colocalization of the peptide with the transvacuolar actin cables. Scale bar = 20 μm.

advantage of peptoids as cell-penetrating agents is their resistance to protease degradation. Peptides, on the other hand, provide a far greater versatility for sequence optimization and a better ease of chemical and recombinant synthesis, the latter aspect being particularly relevant when working with a peptide cargo such as Lifeact. We therefore selected BP100 as a suitable short peptide sequence that is known to be compatible with plants. It was originally designed as an antimicrobial agent against plant pathogens. Here we demonstrate, as a second functionality, its highly efficient uptake into tobacco cells. BP100 is found to exhibit a higher efficiency at much lower concentrations than the cell-penetrating polyguanidine peptoid carriers. Based on this success, if any need for protease-resistance should arise in the future, this could be realized by producing the enantiomeric all-D analogue of BP100, given that this type of peptide operates in a receptor-independent manner at the cellular membrane.[35]

In summary, BP100 has been introduced as an efficient cell-penetrating peptide for plant cells, the first time to our knowledge that actin filaments have been targeted by using a CPP. Peptide constructs with the actin binding peptide Lifeact are thus now available for chemical engineering of the actin cytoskeleton.

Experimental Section

Peptide synthesis: All peptides were synthesized by using standard 9-fluorenylmethoxycarbonyl (Fmoc) solid-phase peptide synthesis.[36] Briefly, Fmoc deprotection was carried out with piperidine (22% *v/v* in DMF), and amino acid coupling was performed in DMF by using a mixture of Fmoc-amino acid/2-(1*H*-benzotriazole-1-yl)-1,1,3,3-tetramethyluronium hexafluorophosphonate (HBTU)/1-hydroxybenzotriazole (HOBt)/*N*,*N*-diisopropylethylamine (DIEA; 4:3.9:4:8 molar ratio). FITC or RhB was used to label the peptides at the N terminus. The resin-bound peptide was labeled with FITC at RT in amine-free DMF, and the mixture was allowed to react overnight. RhB was also coupled at RT but in HOBt/HBTU/DIEA as described above. Peptides were cleaved from the resin by using a solution of trifluoroacetic acid (92%, *v/v*), triisopropylsilane (4%, *v/v*), and water (4%, *v/v*). The peptides were purified by HPLC with acetonitrile/water gradients, as previously described.[37–39] Purified peptides were characterized by analytical liquid chromatography combined with mass spectrometry (LC-MS, for details see the Supporting Information). All peptides were synthesized as C-terminal peptide amides.

Cell lines: The tobacco cell line BY-2 (*Nicotiana tabacum* L. cv. Bright Yellow 2) was cultivated in liquid medium containing Murashige and Skoog salts (4.3 g L^{-1}; Duchefa), sucrose (30 g L^{-1}), KH_2PO_4 (200 mg L^{-1}), inositol (100 mg L^{-1}), thiamine (1 mg L^{-1}), and 2,4-dichlorophenoxyacetic acid (0.2 mg L^{-1}) at pH 5.8.[40] Cells were subcultured weekly by inoculating stationary cells (1.5–2 mL) into fresh medium (30 mL) in 100 mL Erlenmeyer flasks. The cell suspensions were incubated at 25 °C in the dark on an orbital shaker (KS250 basic, IKA Labortechnik) at 150 rpm. Stock BY-2 calli were maintained on media solidified with agar (0.8% *w/v*) and subcultured monthly. The transgenic cell line GF11, which expresses the actin binding domain of plant fimbrin was maintained on the same media supplemented with hygromycin (15 mg L^{-1}).[41] If not stated otherwise, the experiments were performed at three days after subcultivation.

Treatment of cells: For the quantification of uptake, cell suspension (50 μL) and culture medium (950 μL) were mixed in a 1.5 mL reaction tube. If not stated otherwise, fluorescent-labeled BP100 or the 4-kDa FITC-labeled dextrane FD-4 (Sigma–Aldrich) were added to final concentrations of 25 μM (FD-4) and 2.15 μM (BP100). These concentrations had been found during preliminary dose–response studies (data not shown) to be in the linear range without any indications of saturation. The mixture was then incubated with continuous shaking for specified time intervals ranging from 30 min to 20 h. After incubation, the cells were transferred into custom-made staining chambers by using a nylon mesh of 70 μm pore width to allow easy drainage of the fluorescent markers, thoroughly rinsed with sterile culture medium, and viewed immediately.[42] For the quantification of age-dependent uptake, aliquots (50 μL) were taken at different time points after subcultivation and incubated with BP100 or FD-4 for 2 h, as described above. For the inhibitor treatments, stock solutions of latrunculin B (1 mM in DMSO; Sigma–Aldrich), and oryzalin (10 mM in DMSO; Chem Service) were diluted with culture medium to final concentrations of 500 nM (latrunculin B) or 5 μM (oryzalin) and incubated with the cells for 12 h.[43,44] After pretreatment, BP100 or FD-4 was added, and the cells were incubated for 2 h, as described above. To investigate the effects of pH on the uptake, cells were incubated with BP100 or FD-4 in sterile culture medium that had been adjusted to either pH 4.8 or 6.8. After 2 h excess BP100 and FD-4 was removed and the cells were washed in pH-adjusted culture medium, as described above.

 © 2011 Wiley-VCH Verlag GmbH & Co. KGaA, Weinheim

Lifeact: To test whether the fluorescent CPP fusion constructs RhB-Lifeact-BP100 (RLB) or RhB-BP100-Lifeact (RBL; see Figure 5) are able to label actin filaments in vivo, cell suspension (50 μL) and culture medium (950 μL) were carefully mixed in a 1.5 mL reaction tube, and the corresponding peptide was added to a final concentration of 1 μM, and the mixture was incubated for 12 h with continuous shaking. After incubation, the cells were washed, as described above, and directly viewed by fluorescence microscopy. To verify binding to actin filaments in vivo, the tobacco BY-2 cell line GF-11 was used as reference, as it stably expresses a fusion construct of the second actin binding domain (ABD2) of the *Arabidopsis thaliana* AtFim1 protein with GFP.

Microscopy and quantification of uptake: Samples were examined under an AxioImager Z.1 microscope (Zeiss) equipped with an ApoTome microscope slider for optical sectioning and a cooled digital CCD camera (AxioCam MRm). For the observation of RhB, the fluorescence filter set 43 HE (λ_{ex} = 550 nm, beam splitter at 570 nm, and λ_{em} = 605 nm) was used. FITC and GFP fluorescence were viewed through filter set 38 HE (λ_{ex} = 470 nm, beam splitter at 495 nm, and λ_{em} = 525 nm; Zeiss). The images were analyzed by using Axio-Vision (release 4.5) software and processed for publication by using Photoshop (release 5.5, Adobe Systems).

We used the method described previously to quantify the uptake. Briefly, time series of black-and-white images were recorded and analyzed for each time point with the Image J software (http://rsb.info.nih.gov/ij/). Image-acquisition parameters were standardized with respect to time of exposure and adjustment of brightness, contrast and gamma correction to allow for a quantitative comparison of the uptake of BP100 and FD-4. For each individual image, the fluorescence intensity (averaged over the cell interior by using the freehand selection tool of the software) was measured and corrected for background brightness against a reference area outside of the target cell and the initial concentration of fluorophore. For the age-dependent uptake kinetics, the measured intensity value was corrected for cell density because the number of cells per volume increases during progression of the culture cycle. Each data point for the uptake kinetics and the inhibitor treatment experiments represents 136 to 495 individual cells from two to four independent experimental series.

Acknowledgements

This work was supported by the Center for Functional Nanostructures (CFN, TP E1.2 & E1.3), a cluster of excellence by the German Research Council (DFG). Technical support from Sabina Purper in the cultivation of the cell lines is gratefully acknowledged.

Keywords: chemical engineering · CPP · drug delivery · peptides · plant cells · tobacco BY-2

[1] Ü. Langel in *Handbook of Cell Penetrating Peptides,* 2nd ed. (Ed.: Ü. Langel), CRC, Boca Raton, **2006**.
[2] D. Seebach, K. Namoto, Y. R. Mahajan, P. Bindschädler, R. Sustmann, M. Kirsch, N. S. Ryder, M. Weiss, M. Sauer, C. Roth, S. Werner, H.-D. Beer, C. Munding, P. Walde, M. Voser, *Chem. Biodiversity* **2004**, *1*, 65 – 97.
[3] T. Schröder, N. Niemeier, H. F. Krug, S. Afonin, A. S. Ulrich, S. Bräse, *J. Med. Chem.* **2008**, *51*, 376 – 379.
[4] S. B. Fonseca, M. P. Pereira, S. O. Kelley, *Adv. Drug Delivery Rev.* **2009**, *61*, 953 – 963.
[5] C. Foerg, H. P. Merckle, *J. Pharm. Sci.* **2008**, *97*, 144 – 162.
[6] S. Pujals, J. Fernández-Carneado, C. López-Iglesias, M. J. Kogan, E. Giralt, *Biochim. Biophys. Acta Biomembr.* **2006**, *1758*, 264 – 279.
[7] A. Chugh, F. Eudes, *Biochim. Biophys. Acta Biomembr.* **2007**, *1768*, 419 – 426.
[8] A. Chugh, F. Eudes, *J. Pept. Sci.* **2008**, *14*, 477 – 481.
[9] F. Eudes, A. Chugh, *Plant Signal. Behavior* **2008**, *3*, 549 – 550.
[10] M. Mäe, H. Myrberg, Y. Jiang, H. Paves, A. Valkna, Ü. Langel, *Biochim. Biophys. Acta Biomembr.* **2005**, *1669*, 101 – 107.
[11] T. Mizuno, M. Miyashita, H. Miyagawa, *J. Pept. Sci.* **2008**, *14*, 259 – 263.
[12] K. Eggenberger, E. Birtalan, T. Schröder, S. Bräse, P. Nick, *ChemBioChem* **2009**, *10*, 2504 – 2512.
[13] R. Ferre, E. Badosa, L. Feliu, M. Planas, E. Montesinos, E. Bardaji, *Appl. Environ. Microbiol.* **2006**, *72*, 3302 – 3308.
[14] R. Ferre, M. N. Melo, A. D. Correia, L. Feliu, E. Bardaji, M. Planas, M. Castanho, *Biophys. J.* **2009**, *96*, 1815 – 1827.
[15] D. Wade, D. Andreu, S. Mitchell, A. Silveira, A. Boman, H. Boman, R. Merrifield, *Int. J. Pept. Protein Res.* **1992**, *40*, 429 – 436.
[16] H. Kim, M. Park, S. Kim, I. Hwang, *Plant Cell* **2005**, *17*, 888 – 902.
[17] I. Kobayashi, H. Hakuno, *Planta* **2003**, *217*, 340 – 345.
[18] P. Nick, M. Han, G. An, *Plant Physiol.* **2009**, *151*, 155 – 167.
[19] J. Maisch, P. Nick, *Plant Physiol.* **2007**, *143*, 1695 – 1704.
[20] K. Eggenberger, N. Frey, B. Zienicke, J. Siebenbrock, T. Schunk, R. Fischer, S. Bräse, E. Birtalan, T. Nann, P. Nick, *Adv. Eng. Mater.* **2010**, *12*, B406.
[21] J. Riedl, A. H. Crevenna, K. Kessenbrock, J. H. Yu, D. Neukirchen, M. Bista, F. Bradke, D. Jenne, T. A. Holak, Z. Werb, M. Sixt, R. Wedlich-Söldner, *Nat. Methods* **2008**, *5*, 605 – 607.
[22] A. Era, M. Tominaga, K. Ebine, C. Awai, C. Saito, K. Ishizaki, K. T. Yamato, T. Kohchi, A. Nakano, T. Ueda, *Plant Cell Physiol.* **2009**, *50*, 1041 – 1048.
[23] L. Cole, J. Cole, D. Evans, C. Hawes, *J. Cell Sci.* **1990**, *96*, 721 – 730.
[24] P. Campanoni, P. Nick, *Plant Physiol.* **2005**, *137*, 939 – 948.
[25] M. Motizuki, T. Takei, K. Tasaka, S. Yokota, S. Kojima, T. Haga, K. Tsurugi, *J. Biochem.* **2004**, *135*, 713 – 719.
[26] L. C. Morejohn, T. E. Bureau, J. Molé-Bajer, A. S. Bajer, D. E. Fosket, *Planta* **1987**, *172*, 252 – 264.
[27] J. D. Hugdahl, L. C. Morejohn, *Plant Physiol.* **1993**, *102*, 725 – 740.
[28] N. S. Morrissette, A. Mitra, D. Sept, L. D. Sibley, *Mol. Biol. Cell* **2004**, *15*, 1960 – 1968.
[29] I. Spector, N. R. Shochet, Y. Kashman, A. Groweiss, *Science* **1983**, *219*, 493 – 495.
[30] I. Spector, N. R. Shochet, D. Blasberg, Y. Kashman, *Cell. Motil Cytoskel.* **1989**, *13*, 127 – 144.
[31] A. E. Engqvist-Goldstein, D. G. Drubin, *Annu. Rev. Cell Dev. Biol.* **2003**, *19*, 287 – 332.
[32] F. Baluska, J. Samaj, A. Hlavacka, J. Kendrick-Jones, D. Volkmann, *J. Exp. Bot.* **2004**, *55*, 463 – 473.
[33] P. Nick, *Plant Cell Monogr.* **2008**, *143*, 3 – 46.
[34] N. Frey, J. Klotz, P. Nick, *Plant Cell Physiol.* **2009**, *50*, 1493 – 1506.
[35] M. Pritsker, P. Jones, R. Blumenthal, Y. Shai, *Proc. Natl. Acad. Sci. USA* **1998**, *95*, 7287 – 7292.
[36] G. B. Fields, R. L. Noble, *Int. J. Pept. Protein Res.* **1990**, *35*, 161 – 214.
[37] S. Afonin, R. W. Glaser, M. Berditchevskaia, P. Wadhwani, K. H. Guhrs, U. Mollmann, A. Perner, A. S. Ulrich, *ChemBioChem* **2003**, *4*, 1151 – 1163.
[38] P. Wadhwani, S. Afonin, M. Ieromino, J. Buerck, A. S. Ulrich, *J. Org. Chem.* **2006**, *71*, 55 – 61.
[39] P. Wadhwani, J. Bürck, E. Strandberg, C. Mink, S. Afonin, A. S. Ulrich, *J. Am. Chem. Soc.* **2008**, *130*, 16515 – 16517.
[40] T. Nagata, Y. Nemoto, S. Hasezawa, *Int. Rev. Cytol.* **1992**, *132*, 1 – 30.
[41] T. Sano, T. Higaki, Y. Oda, T. Hayashi, S. Hasezawa, *Plant J.* **2005**, *44*, 595 – 605.
[42] P. Nick, A. Heuing, B. Ehmann, *Protoplasma* **2000**, *211*, 234 – 244.
[43] J. Maisch, J. Fišerová, L. Fischer, P. Nick, *J. Exp. Botany* **2009**, *60*, 603 – 614.
[44] K. Schwarzerová, J. Petrášek, K. C. S. Panigrahi, S. Zelenková, Z. Opatrný, P. Nick, *Protoplasma* **2006**, *227*, 185 – 196.

Received: July 14, 2010
Published online on December 14, 2010

 © 2011 Wiley-VCH Verlag GmbH & Co. KGaA, Weinheim